

QUANTUM SIZE EFFECTS IN NANOSTRUCTURES  
AND PROBLEMS OF THERMOELECTRICITY

*D.M. Freik, I.K. Yurchishin, Yu.V. Lysyuk*

*(Institute of Physics and Chemistry, Vasyl Stefanyk Precarpathian National University, 57,  
Shevchenko Str., Ivano-Frankivsk, 76018, Ukraine)*

---

- *This is a review of works dedicated to quantum size effects in low-dimensional materials, specifically: metals, semimetals and semiconductors. Special consideration is given to the ability of a material to achieve a simultaneous power factor increase and thermal conductivity reduction in one direction. Promising semiconductor compounds for the construction of quantum dot, quantum wire, quantum well superlattices and nanostructured composites have been studied.*

**Introduction**

Energy conversion problems are generally known. They have gained a new direction and depth due to intensive nanotechnology developments. Thermoelectricity has not escaped it either. Now we are faced with an acute problem of improving the efficiency of thermal into electrical energy conversion, primarily through use of solid-state thermoelectric modules based on semiconductor compounds. Generators on their basis offer a number of advantages over traditional ones: simple design, absence of movable parts and, hence, noise-free operation and high reliability, possibility of miniaturization without loss of efficiency. However, because of sufficiently low efficiency (6 – 9%) they have not gained wide application, except for in special areas: spacecrafts, ships, electronics, portable refrigerating devices, cooling of infrared sensors, etc [1, 2].

The efficiency of materials used in thermoelectric converters is defined by the value of dimensionless thermoelectric figure of merit:

$$ZT = \frac{\sigma S^2 T}{\kappa} \quad (1)$$

Here  $\sigma$  is electrical conductivity,  $S$  is the Seebeck coefficient,  $\kappa$  is thermal conductivity,  $T = (T_1 + T_2) / 2$  is operating or average temperature, ( $T_1$  and  $T_2$ ) are temperatures of the hot and cold contacts, respectively. Therefore, for the minimization of unproductive expenses of energy in the converters (ohmic and due to thermal conductivity) it is necessary to assure a low thermal conductivity and high values of electrical conductivity  $\sigma$  and the Seebeck coefficient  $S$  of material.

Of practical sense are materials for which  $ZT \approx 1$ . At  $ZT \approx 2 - 3$ , the efficiency  $\approx 20\%$ , which would result in a drastic growth of demand (at  $T = 300$  K), and at  $ZT \approx 3 - 4$  the thermoelectric converters might compete with conventional electric generators. The Seebeck coefficient and electrical conductivity are governed only by electron subsystem ( $P = S^2 \sigma$  is power factor). The thermal conductivity is governed by the electron and phonon subsystems ( $\kappa = \kappa_e + \kappa_L$ ). The values  $\kappa_e$  and  $\sigma$  are interrelated by the Wiedemann-Franz law

$$\frac{\kappa_e}{\sigma} = L_0 T \quad (2)$$

where  $L_0$  is the Lorentz constant. In so doing, the electrical conductivity increase is followed not only by growth of  $\kappa_e$ , but also by a reduction of coefficient  $S$ .

In the bulk samples, the main method for improving power factor  $P = S^2 \sigma$  is doping, and the

method for reducing thermal conductivity  $\kappa$  is selection of optimal alloy components. Over the course of the past half a century no essential results have been achieved in reaching the necessary  $ZT$  values. Thus, for the room temperature range one profitably employs the alloys based on bismuth and antimony tellurides, for the temperatures (500 – 700) K – lead telluride (Fig. 1) [3, 4]. There is certain outlook for composite alloys based on germanium, silver and cobalt (Fig. 2) [5].

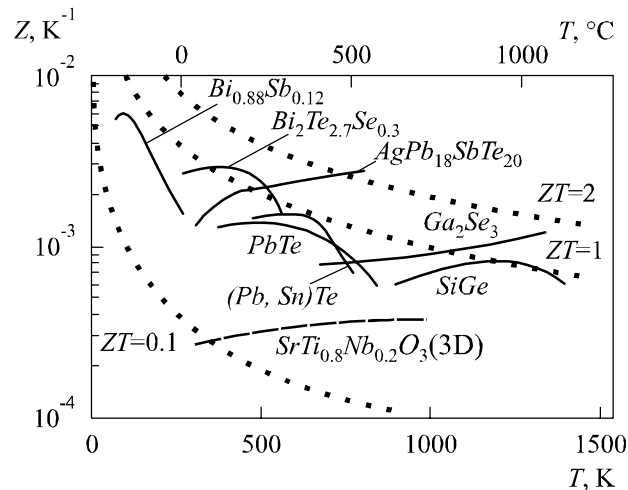


*Fig. 1. Thermoelectric figure of merit of promising materials as a function of temperature [2].*

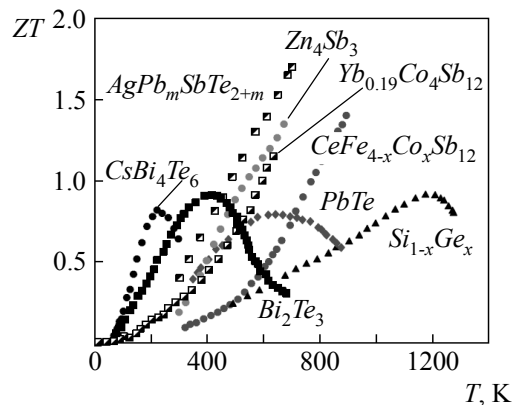


*Fig. 2. Dimensionless thermoelectric figure of merit of promising materials as a function of temperature [5].*

In recent years, a new line has emerged for improving the thermoelectric characteristics of materials where progress has been achieved and which has given a new impetus to corresponding research in this field. This approach lies in the use of spatially inhomogeneous structures with inclusions that are comparable in size with characteristic wavelength of electrons and phonons, that is, they are in nanometer region. A reduction of system dimensions to nanometer scale causes drastic differences in the density of electron states (Fig. 3), creating new possibilities for quasi-independent variation of  $S$ ,  $\sigma$  and  $\kappa$ . The nanosized components create a quantum size effect which improves power factor  $S^2\sigma$ , and the arrangement of internal boundaries in a nanostructure allows reducing thermal conductivity as compared to electrical conductivity which is based on the differences between the phonon and electron scattering lengths. On this basis, systems with quantum wells, wires and dots, as well as various components with disordered nanosized inclusions are created.

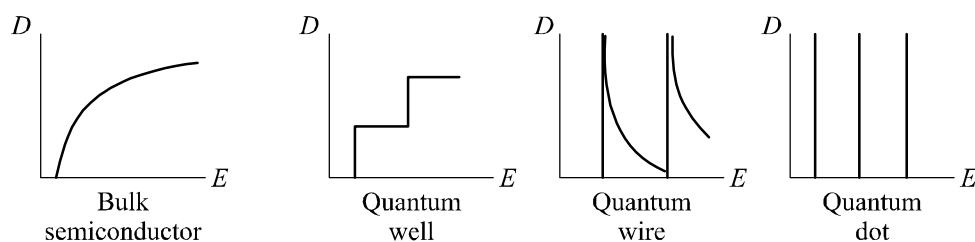


Fig. 3. Density of states versus energy for the bulk samples, quantum wells, wires and dots [1].

Our purpose in this work is a review of research on the thermoelectric properties of nanostructured materials.

## 1. Strategies and concepts for thermoelectric performance enhancement

Theoretical test of a model of two-dimensional periodic quantum well system [5], and then single-dimensional quantum wire system [6] and their subsequent experimental validation [7, 8] enabled introduction of two strategies in the field of low-dimensional thermoelectricity:

- use of quantum size effects for the Seebeck coefficient increase and independent control of  $S$  and  $\sigma$  values;
- introduction of a considerable number of boundaries that scatter phonons more efficiently than electrons, as well as scatter preferably those phonons that contribute to thermal conductivity most of all.

The ability of a system of low-dimensional materials to enhance the thermoelectric (TE) figure of merit was first demonstrated for  $PbTe$  quantum well superlattice with  $n$ -type  $Pb_{1-x}Eu_xTe$  barriers [7] and later on for a similar  $p$ -type superlattice [9]. In so doing, a good agreement was obtained between the theoretical and experimental dependence  $S^2n$  on the well width (dependence structure  $S^2n$  rather than  $S^2\sigma$  is due to the fact that  $n$  and  $\sigma$  are related by the formula  $\sigma = ne\mu$ , where  $e$  is electron charge,  $n$  is concentration of carriers, and their mobility  $\mu$  is very sensitive to ambient factors, such as defects, whereas  $S^2n$  is more closely related to the internal parameters of materials). The increase in  $S^2n$  was demonstrated not only for  $PbTe$  semiconductor superlattices, but also for  $Si$  quantum wells in  $Si/SiGe$  systems [10], where a good agreement between theory and experiment was also achieved. Experimental research on the transverse transport in  $Bi_2Te_3/Sb_2Te_3$  superlattices has shown that phonon scattering on the boundaries has reduced thermal conductivity to a larger extent than electrical conductivity [11, 12], thereby proving the criticality of the second strategy that assures larger  $ZT$  growth compared to the case when  $ZT$  increase is due to increase in  $S^2n$ .

Upon the experimental validation of the above strategies, investigations are pursued in two different lines. In the first line, the efforts aim at achieving progress in the design and growth of superlattices, in the second – at obtaining ordered structures of smaller size (single-dimensional quantum wires and 0-dimensional quantum dots). The use of low-dimensional materials for thermoelectric figure of merit enhancement has obtained more scope due to the use of the following concepts: energy throttling of carriers on barriers; "carrier-pocket" engineering; semimetal- semiconductor transition. Note that all these concepts and strategies are currently used to improve the efficiency of nanostructured thermoelectric materials in the course of basic and applied research in this field.

### 1.1. Energy throttling of carriers on barriers

The concept of energy filtration of carriers is introduced for increasing the thermoelectric power factor  $S^2\sigma$  and consists in the introduction of respective barriers in the form of boundaries that restrict

the energy of carriers entering the material. Carriers with the average energy considerably higher than the Fermi level  $E_F$  will preferably pass through the boundary. It will improve the Seebeck coefficient which depends on the excess energy ( $E - E_F$ ) of carriers in a sample. Procedure of introducing additional barriers will lead to a reduction of conductivity  $\sigma$ , which in this approach is well compensated by growth of  $S$ . Thus, energy filtration process leads to growth of  $S^2\sigma$  [12, 13].

### **1.2. "Carrier-pocket" engineering**

The essence of "carrier-pocket" engineering [14] lies in the development of superlattice structure in such a manner that one carrier type is quantum restricted in the area of a quantum well, and the other carrier type of the same sign – in the area of a barrier. This concept was introduced for the case of electron  $\Gamma$ -point of *GaAs* quantum wells and for electron  $X$ -point of *AlAs* barriers [15] in *GaAs/AlAs* quantum well superlattices [14]. It is also used for 2-dimensional *Si/SiGe* superlattices [16] and, in a sense, in self-organized nanostructured composites.

### **1.3. Semimetal-semiconductor transition**

The concept of semimetal-semiconductor transition is primarily concerned with bismuth and its related materials. Although *Bi* possesses high Seebeck coefficient at electron  $L$ -point [15], the fact that it is a semimetal and, accordingly, has both charge carriers – electrons and holes, leads to a reduction of  $S$ . Conversion of bismuth semimetal into  $n$ -type semiconductor can be done by using low-dimensional structures on its basis or alloys with antimony. Development of two-dimensional superlattices based on *Bi* quantum wells is impeded by the difficulty of seeking for a suitable barrier material. Therefore, low-dimensional materials based on *Bi* and  $Bi_{1-x}Sb_x$  alloys are used as ordered series of 1-dimensional quantum wires inside the pores of anodic aluminum samples [17]. When we speak about the mechanism of semimetal-semiconductor transition, with a reduction of wire diameter there occurs splitting of energy levels into separate subbands, which is attended with motion of the edge of the lowest conduction subband upstream and the edge of the highest valence subband downstream the energy. When these energy levels intersect, the material makes a transition from a semimetal to semiconductor with a certain energy gap [17 – 19]. To achieve considerable domination of one carrier type in the semiconductor phase, the material can be doped. Such semimetal-semiconductor transition had been predicted [20] and later observed experimentally for *Bi-Sb* nanowires [20, 21].

## **2. Quantum size effects**

What is called quantum size effect is a dependence of thermodynamic properties and kinetic coefficients of solids on their characteristic dimensions when the latter become commensurate with the effective de Broglie wavelength of elementary excitations. Current interest in studying quantum size effects is caused by intensive progress in the field of nanotechnologies. The theoretical groundwork for quantum size effects was laid in the works of 50-60-s by Lifshits, Kosevich, Sandomirsky, Tavger and Demikhovskiy [22 – 28], and a report on their experimental validation appeared in 1966 (Ogrin, Lutsky and Elinson) [29, 30] and dealt with bismuth thin films whose properties were studied in a wide range of thicknesses. With regard to complexity of effect observation in actual films, the experimental achievements proved to be much more modest than theoretical predictions. Initially the works on quantum-size effect most often discussed the situation when only one subband with a square law of dispersion is occupied. Such a model was used for the calculation of electrical conductivity and galvanomagnetic properties of size-quantized semiconductor and semimetal films [31]. Developing the theory of quantum size effects, V.B.Sandomirsky in 1967 by an example of isotropic semimetal

assumed that charge carrier scattering in it occurs on  $\delta$ -like potential and obtained a saw-tooth like relaxation time function of energy [32]. Thus, the works on the calculation of thickness dependences ( $d$ ) of TE parameters of thin films are related to calculation of relaxation time, as well as the thickness of states for different conditions. Oscillation of density of states versus the thickness of films governs the oscillations of the respective TE parameters. The density of states depends on the Fermi energy of system which accounts for a large number of works dedicated to calculation of this energy characteristic [33].

V.B. Sandomirsky showed that the presence of a finite minimum energy determined by film thickness [32] is the reason for reduction of overlapping in semimetals, and at certain thickness  $d_0$  can result in semimetal-semiconductor transition [34]. In a model of a rectangular well with infinitely high walls for isotropic semimetal the thickness  $d_0$  coincides with oscillation period  $\Delta d$ . In work [33] the critical thickness of transition is calculated for said model with different orientations of bismuth and antimony films. In 1982 the authors of [35] observed experimentally the semimetal-semiconductor transition with a change in thickness of bismuth-antimony alloy. Thus, for instance, for  $Bi_{0.83}Sb_{0.17}$  films it occurs with the thickness of 7 – 8  $\mu\text{m}$ . Now work is underway to establish such a transition for pure bismuth films.

Quantum size effect is also investigated through use of tunneling spectroscopy. G.A. Gogadze and I.O. Kulik in 1965 showed that tunneling current from a size-quantized film is an oscillating bias function which reflects the peculiarities of density of states [36]. It was also shown that conductivity of tunneling system with a change in film thickness is monotonously changed, the regions of fast and slow drop of conductivity being alternated [36, 37].

For practical observation of quantum size effect it should be taken into account that the structure and electronic properties of thin films are largely governed by technological factors (the type and temperature of substrate, batch composition, interaction with oxygen, etc), which necessitates study of the effects of these factors on the manifestation of oscillation effects. The theoretical works, as a rule, are concerned with an idealized model of single-crystal film with mirror smooth surfaces. The presence of defects in the bulk of the film and surface roughness lead to a reduction of amplitude of quantum size oscillations [38]. Work [39] discusses a change in the character of electron-phonon scattering in a quantized film which is due to the presence of surface. When electrons interact with impurities, the thickness dependences of TE parameters with a size quantization become rather complicated though retain their oscillating character [40].

## **2.1. Conditions of the existence of quantum size effects in nanostructures**

The proportionality between de Broglie wavelength and the characteristic dimensions of nanostructures generally exists in semimetal and semiconductor structures. There are also certain requirements to experimental conditions and material structure. Let us consider these conditions by an example of a thin film.

As can be seen from Fig. 4, the spectrum of carriers in a film is composed of bands that are overlapped. In so doing, the specific feature of film spectrum is the availability of finite minimum energy  $\varepsilon_1$ . When current carriers occupy a large number of these bands, spectrum quantization should not be of essential importance. Dimensional quantization can become apparent only in the case when the average energy of conduction electron  $\bar{\varepsilon}$  is of the same order as characteristic quantization energy  $\varepsilon_1$  [41, 42]:

$$\varepsilon_1 \equiv \varepsilon(n=1, \kappa_x = \kappa_y = 0) = \frac{\hbar^2 \pi^2}{2m_{\perp} d^2}, \quad (3)$$

where  $n$  is dimensional quantum number;  $m_{\perp}$  is effective mass of current carriers in direction

perpendicular to film area;  $d$  is its thickness. That is, carriers should occupy a small number of subbands (a subband in this case should be understood to mean the values acquired by energy  $\varepsilon$  under given value of quantum number  $n$ .) Hence, a prerequisite for quantum size effect manifestation is:

$$\bar{\varepsilon} \approx \frac{\hbar^2}{2m_{\perp}} \frac{\pi^2}{d^2} \text{ or } d \approx \frac{\pi\hbar}{\sqrt{2m_{\perp}\bar{\varepsilon}}} \approx \lambda_D, \quad (4)$$

where  $\lambda_D$  is de Broglie wavelength. In condition (4) for the degenerate electron gas  $\bar{\varepsilon}$  is of the same order as the Fermi energy  $\zeta_F$ , and for the nondegenerate  $\bar{\varepsilon} \approx k_0T$ . Thus, for the manifestation of dimensional quantization, film thickness must be commensurate with the de Broglie wavelength  $\lambda_D$  for carriers. From (4) it is also evident that manifestation of quantum size effect at real thicknesses requires a low effective mass, small filling of spectrum or low temperatures. Calculations by formula (4) yield unreal thicknesses for metal films and real ones for semiconductor and semimetal films.

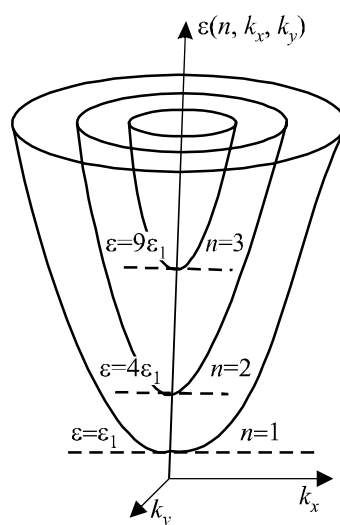


*Fig. 4. Partially quantized spectrum of current carriers in a thin film [41].*

The process of current carrier scattering leads to partial blurring of quasi-discrete spectrum by the value  $\hbar/\tau$ , where  $\tau$  is relaxation time. To retain spectrum discreteness, the following condition should be met:

$$\frac{\hbar}{\tau} \ll \varepsilon_{n+1} - \varepsilon_n, \quad \frac{\hbar}{\tau} \ll (2n+1)\varepsilon_1, \quad (5)$$

In (5) the second condition follows from the first one due to a replacement  $\varepsilon_n = \varepsilon_1 n^2$ . Condition of quasi-discrete spectrum existence in film (5) is most strict and is satisfied only in rather perfect and pure films where carriers have a long mean free path. A directly proportional relation between the mobility and relaxation time  $\mu = e\tau/m$  imposes the following condition on it

$$\mu \gg \frac{ed^2}{\pi\hbar} \quad (6)$$

Besides, the film must be thickness homogeneous, so that a change in position of size levels in its different portions due to accidental thickness variation is considerably less than the distance between them. For this purpose a relative thickness variation should satisfy the condition [41]:

$$\frac{|\Delta d|}{d} \ll \frac{(2n+1)}{2n^2} \quad (7)$$

where  $n$  is subband number. With relatively high  $n$ , as can be seen from (7), thickness variation  $|\Delta d|$  should be smaller than  $d/n$ , to avoid overlapping of film subbands of different areas. The film

thickness homogeneity is also necessary to assure mirror scattering of carriers from the surface, when quasi-impulse projection reflected from the surface is not changed. For this purpose the inhomogeneity size  $|\Delta d|$  must be smaller than the de Broglie wavelength for current carriers.

To observe the oscillation quantum size effects, current carriers in a film must be degenerate  $k_0T \ll \zeta_F$ , and blurring of the Fermi distribution (the Fermi boundary) must be much smaller than the distance between the neighbouring subbands [41, 42]:

$$k_0T \ll (2n+1)\varepsilon_1 < \zeta_F \quad (8)$$

The latter inequality in (8) highlights the fact that for the observation of oscillation quantum size effects there must be at least several film subbands under the Fermi level.

Thus, in general for nanostructures one can state that realization of quantum size effects requires materials with a low effective mass of carriers, low occupancy (the Fermi level), high mobility and mirror surface scattering (thickness homogeneity), and it is desirable to conduct the experiments at low temperatures (8).

## **2.2. Quantum size effects in metals, semimetals and semiconductors**

As previously discussed, the above conditions for realization of quantum size effects are best met by semimetal and semiconductor structures. However, this does not preclude the necessity of studying quantum size effects in metals, because metallic inclusions are an important component of up-to-date nanostructured materials (for instance, metallic inclusions in a semiconductor nanocomposite array or aluminum templates of *Bi* nanowires).

In 1968 the authors of [43] discovered in tin thin films the Blatt-Thomson effect which lied in the fact that with a change in film thickness the critical temperature and superconducting gap oscillated with damping amplitude. The effect was theoretically explained by the nonmonotonic dependence of density of states on film thickness. The oscillation period was equal to the de Broglie half-wavelength.

In work [44], in the range of liquid helium temperatures (4.2 K), the presence of little oscillations of aluminum film transparency is shown as a thickness function. A rise in temperature to liquid nitrogen value has resulted in oscillation amplitude reduction and its complete disappearance at room temperature. According to authors' prediction the obtained nonmonotonic variation of transparency versus thickness is a result of quantization. Aluminum forms a good optical surface capable of mirror reflection of electrons, and spin-orbit interaction that causes blurring of quantization effect is very slight in it [44]. Therefore, the nonmonotonic change in transparency can really result from quantization, and oscillation amplitude reduction with a rise in temperature can occur due to reduction of mean free path of electrons. Important conclusions as to the possibility of quantum size effect demonstration in gold films were made by the authors of [45]. Due to a low value of the de Broglie wavelength and, respectively, low oscillation period, for their growth one should use specific technological means or, the so-called surfactant substrates (for instance, with a sublayer of *Bi<sub>2</sub>O<sub>3</sub>*, *Al*, *Ge*, etc.). The size dependences of copper films resistivity ( $d \approx 4 - 30$  nm), sputtered in high vacuum ( $10^{-7}$  Pa) even at low temperatures (78 K) show no oscillations. The unobservability of oscillations was explained by the presence of surface inhomogeneities and peculiarities of film growth dynamics [46]. Therefore, manifestation of dimensional quantization in metals should be observed when the size of respective inclusion becomes less than 4 – 5 nm, since exactly these dimensions are commensurate with the de Broglie wavelength of current carriers. In the case of thin metal films, to obtain homogeneous continuous layers of such small thicknesses it is necessary to overcome a number of technological problems.

As regards quantum size effects in semimetals, the best studied in this area is bismuth. Thus, thickness dependences of resistance, the Hall coefficient, magnetoresistance, as well as concentrations

for bismuth thin films on mica at 300, 78 and 4.2 K are of oscillation type with approximately the same period ( $\Delta d = 400 - 500 \text{ \AA}$ ) and oscillation amplitude [29, 47]. At room temperatures, oscillations are essentially smoothed out as compared to low temperatures. In so doing, structural characteristics of *Bi* epitaxial films on mica testify to their high perfection [48]. The results were explained by dimensional quantization.

According to theoretical calculations of V.B. Sanomirsky [32], the  $d$ -dependence of bismuth thin films is an oscillating function that coincides with thickness reduction. At the same time, the authors of [49] at low temperature (4.2 K) observed an anomalous size effect characterized by the fact that in polycrystalline bismuth thin films conductivity grows with a reduction of their thickness. Such an anomalous dependence can be explained by growth of film structural perfection, but it is nearly impossible with a reduction of thickness. The authors of [49] attributed this run of the curve  $\sigma(d)$  to growth of hole and electron relaxation time with a decrease in film thickness. Growth of relaxation time leads to growth of mobility and conductivity of carriers. Much later [50] the same authors showed that doping of bismuth films with antimony (4 at.%) results in the average resistance growth over the entire range of investigated thicknesses, as well as in the growth of its amplitude and oscillation period from  $\sim 260$  to  $650 \text{ \AA}$ , that is, more than twice. Such results allowed making a principal conclusion that in structurally perfect bismuth films the resistance oscillations are related exactly to spectrum parameters, and not to some other accidental reasons.

The run of the electrical conductivity oscillation dependence on the thickness of antimony thin films is in full agreement with the respective theoretical dependence of V.B. Sandomirsky [32], namely the electrical conductivity drops with a decrease in thickness [51]. This marks it off qualitatively from the respective dependence for bismuth films with the anomalous size effect. Reduction of  $\sigma$  in antimony films can be related to degradation of structural characteristics of films with a decrease in thickness, as testified by amplitude reduction and quantum oscillation blurring.

The authors of [52] have demonstrated for bismuth films that oscillation amplitude depends on their structural perfection and, as a rule, is larger for areas close to maximum thickness, where quality of films is higher due to a perpendicular drop of a molecular beam. According to experimental data, the oscillation amplitude for films less than 100 nm thick with a decrease in thickness is markedly reduced instead of considerable growth expected by theory. The authors assumed that damping of oscillations is related to spectral deformation close to surface due to the influence of surface states.

In [30], tunneling spectroscopy method was used to evaluate the Fermi energy in bismuth film within  $(0.02 \div 0.027) \text{ eV}$ , as well as the effective mass of electrons in *Bi*  $m_{efBi} \sim 0.012m_0$ . As can be seen, the Fermi energy values in *Bi* films are close to known Fermi energy values in the bulk bismuth, and measurement of effective mass by tunneling spectroscopy method is in good agreement with the known value of this quantity from measuring de Haas-van Alphen effect. In work [53], for *Bi* films on *KBr* substrates there was revealed a displacement of optical absorption red boundary with a change in film thickness, that is, a change in the energy gap width, which is a consequence of quantum size effect.

According to [54], a decisive influence on the oscillation dependences of kinetic coefficients on the thickness of *Bi* films evaporated in vacuum on mica substrates is produced by substrate temperature in the course of growing. Thus, a reduction of substrate temperature from  $T_n = 380 \text{ K}$  to room temperature leads to smoothing out the oscillations and reducing maximum values of kinetic coefficients. This effect is attributable to a higher degree of structural perfection of films grown at a higher substrate temperature. Besides, this work highlights growth of all kinetic coefficients with increasing film thickness to  $\sim 200$  with a subsequent attainment of saturation. It is assumed that critical thickness of *Bi* films which corresponds to "semimetal-semiconductor" transition is  $d = 25 \pm 5 \text{ nm}$ .

Quantum size effect in the field of semiconductor materials is characterized by the largest number of works, especially as regards IV – VI compounds. A good many of these works are not only of scientific, but also of applied importance, so the main emphasis on these papers will be placed in the next section of this review.

One of conditions for observation of quantum size effect in semiconductors is electron gas degeneracy. Experimental and theoretical studies show that in semiconductor thin films the energy spectrum of electrons is of quasi-discrete nature. A low density of states in conduction band leads to electron gas degeneracy in it. Thus, dependences of electrical resistivity  $\rho$ , the Hall coefficient  $R_H$ , mobility  $\mu = R_H/\rho$  on thickness  $d$  of  $n$ -type  $Sb$  films are of oscillation type. At  $d \leq 300 \text{ \AA}$  one can see a drastic growth of  $\rho$  which is mainly caused by carrier concentration decrease. The authors interpret this effect as removal of electron gas degeneracy [55].

Oxidation processes occurring in thin film structure produce a very serious effect on its properties. Thus, in our earlier works [56, 57] and in the works by E.I. Rogacheva it was shown that oxygen effect on lead chalcogenide thin films causes growth of  $n$ -type carrier concentration in them. Finally, in the initially  $n$ -type films this leads to the inversion of predominant carrier sign from  $n$  to  $p$ . Based on the results of works [58 – 61] it can be said that coating of films with a thin layer of  $EuS$  ( $\approx 30 \text{ nm}$ ) protects them completely from oxidation. In these works, oscillations of thermoelectric parameters in IV-VI  $PbSe$ ,  $PbS$ ,  $PbTe$  thin films are investigated. The  $KCl$  substrate (mica for  $PbTe$ ) and  $EuS$  surface layer ( $Al_2O_3$  for  $PbTe$ ) provided a quantum well for carriers in the film layer. Estimation of oscillation period  $\Delta d$  of TE parameters by the known value of charge carrier effective mass and the Fermi energy ( $\epsilon_F$ ) demonstrates a good agreement with the experiment for  $PbTe$  QW, and a fuzzy match with the experiment for  $PbSe$ ,  $PbS$  QW. Such a mismatch in the experimental and theoretically calculated oscillation period is attributed by the authors to simplifications in the employed model, namely to isotropy and parabolicity of conduction band, mirror scattering of charge carriers, identity and infinite height of quantum well walls. Comparison of  $d$ -dependences of TE parameters of nanostructures of stoichiometric and with 2 at.% lead excess (001)  $KCl/PbTe/EuS$  has shown that lead excess results in growth of  $n$ -type carrier concentration, increase of maximum value of thermoelectric power factor  $S^2\sigma$ , as well as displacement of maxima of oscillation dependences  $\sigma(d)$  and  $S^2\sigma(d)$  to the right toward a larger thickness of  $PbTe$  condensate, and for  $S(d)$  – to the left [62]. Thus, a change in charge carrier concentration preserves general oscillation character of  $d$ -dependences of thermoelectric parameters in quantum wells of  $KCl/PbTe/EuS$  nanostructure, though the extreme positions in this case are displaced.

A good agreement between the experimental and theoretical oscillation period in QW model with infinite walls is observed in the dependences of TE parameters on the thickness of  $p$ - $SnTe$  layer in  $KCl/n$ - $PbTe/p$ - $SnTe/n$ - $PbTe/EuS$  heterostructure. In so doing, the thicknesses of the lower and upper  $PbTe$  layers were kept constant ( $d^1_{PbTe} \approx 40 \text{ nm}$  and  $d^2_{PbTe} \approx 10 \text{ nm}$ ), and the thickness of  $SnTe$  layer varied within  $d_{SnTe} = (0.5 - 6.) \text{ nm}$  [63].

The  $d$ -dependences of TE parameters of nanostructures  $p$ - $SnTe$  [64, 65],  $PbTe:Bi$  [66] on mica and  $PbTe$  on polyamid [67] without the external protective layer are also of oscillation nature. In this case quantum well for carriers is realized due to two barriers: the substrate and the layer on structure surface strongly enriched in acceptor centers. In the case of a polycrystalline structure oxygen diffusion can be attended with formation of a thin absorbed layer on the surface of each nanocrystallite; then quantization of the energy spectrum of carriers will occur within each crystallite. The authors of the above mentioned works note that maxima in the  $d$ -dependences of electrical and kinetic parameters are also governed by the mechanisms of condensate growth.

### 3. Nanostructured thermoelectric materials

In semiconductor nanomaterial research three basic nanoobjects are introduced: two-dimensional quantum wells, single-dimensional quantum wires and zero-dimensional quantum dots. Based on these three objects, superlattices and composites of various types are being designed today. Calculations show that changing the characteristic size of quantum wells, wires and dots, one can increase considerably the values of thermoelectric power factor  $P = S^2\sigma$  and thermoelectric figure of merit  $ZT$ . It is primarily due to the fact that size reduction leads to a change in the electron density of states.

#### 3.1. Superlattices

Experimental validation of the possibility of increasing the Seebeck coefficient on which the basic hopes related to low dimensional systems had been initially pinned was demonstrated in  $PbTe/Pb_{1-x}Eu_xTe$  QW superlattices [7]. Using a molecular beam epitaxy method, on (111)  $BaF_2$  substrates one first grew a buffer layer  $PbTe/Pb_{0.958}Eu_{0.042}Te$  200 nm thick, and then  $PbTe/Pb_{0.927}Eu_{0.073}Te$  QW superlattice proper with the number of periods from 100 to 150. The thicknesses of  $PbTe$  layers varied between 17 and 55 Å, and the thickness of  $Pb_{0.958}Eu_{0.042}Te$  barrier layers was nearly 450 Å. Carrier concentration was varied with the use of Bi donor atoms in barrier material. By this means,  $n$ -type conduction was achieved in quantum well conduction band. Measurement of resistivity, the Hall and Seebeck coefficients was carried out in the direction parallel to superlattice layer planes at 300 K. As a result, growth of TE power was recorded with a reduction of  $PbTe$  layer thicknesses and increase of  $n$ -type carrier concentration (Fig 5). It was also experimentally shown that the Seebeck coefficient of single  $PbTe$  QW with  $Pb_{0.958}Eu_{0.042}Te$  barriers is equal to  $S$  of a sample of multiple quantum wells. In so doing, the experimental points for TE power  $S^2n$  fell rather well on the theoretical curve for  $PbTe/Pb_{0.927}Eu_{0.073}Te$  QW (Fig. 5).

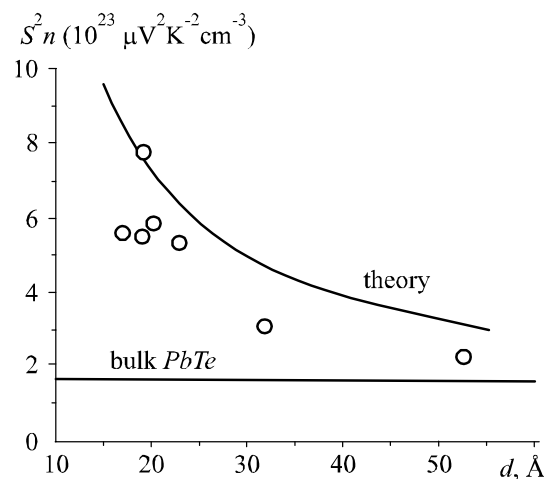


*Fig. 5. Experimentally found coefficient  $S^2n$  for  $PbTe/Pb_{0.927}Eu_{0.073}Te$  QW superlattices as a function of  $PbTe$  layer thickness at  $T = 300$  K. Continuous line represents a theoretical model [7].*

An important feature of superlattices is their ability to reduce lattice thermal conductivity as compared to the bulk materials. Selective transmission of high-frequency phonons is observed in direction transverse to layer thickness [68]. Thus, thermal conductivity of  $Si/Ge$  QW superlattices with the period (130 – 300) Å has the value close to  $2 \text{ W} (\text{m}\cdot\text{K})^{-1}$ , that is half as large as that of  $Si_{0.85}Ge_{0.15}$  alloy films with thermal conductivity  $(4 - 5) \text{ W}(\text{m}\cdot\text{K})^{-1}$ . Besides, a decrease in period value of such a superlattice leads to growth of lattice thermal conductivity [69]. The same halving of thermal conductivity in a direction perpendicular to layers was observed in  $Bi_2Te_3/Sb_2Te_3$  QW superlattices

with periods (40 – 120) Å [70], which is supported theoretically [71].

Theoretical calculations show that in superlattices with a complex structure of unit cell where each period consists of three, four and larger number of layers, a more essential reduction of thermal conductivity is possible [72, 73]. A record-breaking value of thermoelectric figure of merit  $ZT = 2.4$  was observed in *p*-type  $Bi_2Te_3/Sb_2Te_3$  QW superlattices at 300 K with  $Bi_2Te_3$  and  $Sb_2Te_3$  layer thicknesses 10 and 50 Å, respectively. In so doing, lattice thermal conductivity was  $0.22 \text{ W}(\text{m}\cdot\text{K})^{-1}$ , and superlattice structure itself had no effect on the hole mobility that was identical along and across the layers and almost twice exceeded the hole mobility in  $BiSbTe_3$  alloy. In *n*-type  $PbTe/PbTe_{0.75}Se_{0.25}$  QW superlattices with a high electron concentration ( $10^{19} \text{ cm}^{-3}$ ), grown by thermal evaporation in vacuum, there is also a twofold thermal conductivity reduction as compared to films of  $PbTe_{0.75}Se_{0.25}$  alloy to  $0.5 \text{ W}(\text{m}\cdot\text{K})^{-1}$ . The TE figure of merit for such a superlattice is  $ZT = 0.63$  at 300 K in a direction perpendicular to layers and  $ZT = 1.75$  at 425 K – parallel to layers, exceeding considerably the respective values for the bulk  $PbTe$ .

New technological procedures, in particular, molecular-beam epitaxy and realization of the Stranski-Krastanov growth mechanism enabled creation of quantum dot structures. Until recently, optoelectronics has been considered the main area for application of quantum dot arrays. Starting from 2000, the theoretical and experimental works came out that stipulated possible major increase in thermoelectric figure of merit in superlattices and proved it experimentally [74, 75]. The value of such superlattices lies in a simultaneous realization of two strategies: phonon scattering on the flat layers of randomly distributed quantum dots without essential effect on the electron subsystem, as well as increase of power factor  $S^2\sigma$  due to quantum size effects.

The foregoing is confirmed in work [76]. On  $BaF_2$  substrates, using a molecular-beam epitaxy method,  $PbSe_{0.98}Te_{0.02}/PbTe$  QD superlattices of thickness 100 μm and size  $(1.8 \times 1.8) \text{ cm}^2$  were grown. Typical sample of such a superlattice was composed of 8005 periods, 13 nm thick each. In so doing, due to doping with bismuth, from the source of  $Bi_2Te_3$  effusion cell there were obtained *n*-type QD superlattices. In fact, quantum dots were formed in  $PbSe_{0.98}Te_{0.02}$  layers. By changing the level of doping and growth parameters, there were obtained 15 samples of  $PbSeTe/PbTe$  QD superlattices with different thermoelectric figure of merit  $ZT$  and the Seebeck coefficient  $S$  (Fig. 6) [76]. It can be seen that the Seebeck coefficient growth attends the increase in  $ZT$  value from  $\sim 1.4$  to  $\sim 1.7$ . For a sample with the highest  $ZT$  in nitrogen atmosphere at pressure  $\sim 1$  atm there was revealed a predominance of metallic behaviour (growth) of resistivity with temperature over the increase of the Seebeck coefficient, which is the reason for reduction of  $S^2\sigma$  value (Fig. 7). Note also that in 2002 the authors of [76] reported on  $ZT = 2$  at 300 K in  $PbTe/Pb_{1-y}Sn_yTe_{1-x}Se_x$  QD superlattices with  $x = 98\%$ ,  $y = 16\%$  [77].

Let us consider in more detail the mechanisms responsible for these results. First, for  $PbSeTe/PbTe$  QD superlattices a drastic reduction of lattice thermal conductivity ( $\kappa_L$ ) gives the value of general thermal conductivity in the range of  $(0.58 - 0.62) \text{ W}(\text{m}\cdot\text{K})$  [77]. Evaluation of electron thermal conductivity  $\kappa_E$  together with the use of the Wiedemann-Franz law allows obtaining  $\kappa_L \approx 0.33 \text{ W}(\text{m}\cdot\text{K})$  (still lower values are possible in a quaternary  $Pb_{0.84}Sn_{0.16}Se_{0.98}Te_{0.02}/PbTe$ ) QD superlattice. With regard to the fact that lattice thermal conductivity of equivalent disordered alloy  $PbSeTe$   $\kappa_L \approx 1.25 \text{ W}(\text{m}\cdot\text{K})$ , it can be said that the effect of quantum dots lies in reducing  $\kappa_L$  almost by a factor of 4, and, possibly, even more for a quaternary QD superlattice. On the other hand, up to concentration  $2 \cdot 10^{19} \text{ cm}^{-3}$  the mobility of carriers in lead chalcogenides is weakly dependent on doping level [77]. Another mechanism responsible for  $ZT$  increase in QD superlattices lies in growing the Seebeck coefficient which proves to be higher than in the bulk materials with the same density of

carriers. In  $Pb_{0.98}Sn_{0.02}Se_{0.13}Te_{0.87}$  QD superlattices with a mobility higher than  $500 \text{ cm}^2/(\text{V}\cdot\text{s})$  the thermoelectric power factor  $S^2\sigma$  is rather high. The task of further theoretical efforts is to explain such a behaviour which, apparently, is related to quantum-size effects.

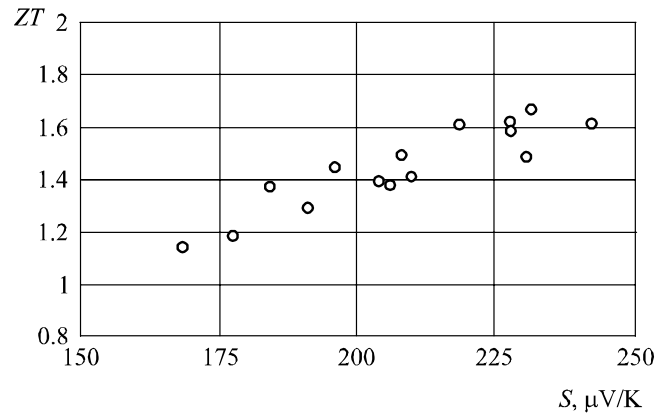


Fig. 6. Dependence of thermoelectric figure of merit on the Seebeck coefficient for different samples of n-type  $PbSe_{0.98}Te_{0.02}/PbTe$  QD superlattices at 300 K [76].

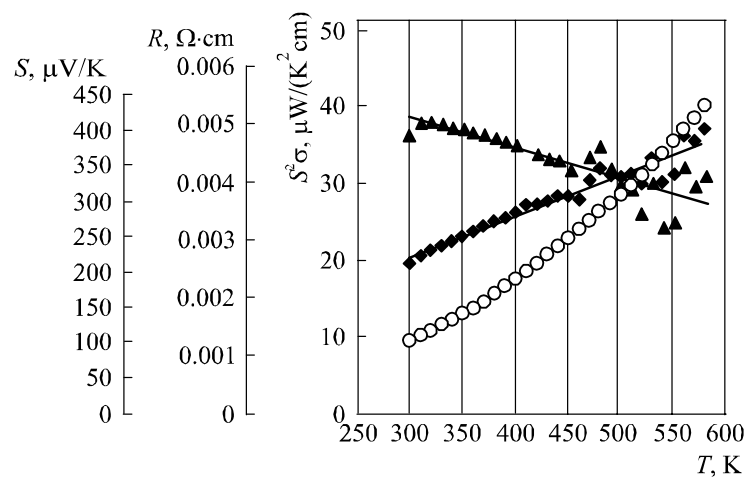


Fig. 7. Dependence of the Seebeck coefficient (rhombus), electrical resistivity (circles) and power factor (triangles) on temperature for different samples of n-type  $PbSe_{0.98}Te_{0.02}/PbTe$  QD superlattices at 300 K [76].

Theoretical calculations also show that in the case of meeting the conditions for formation of minibands in *Ge* QD superlattices in *p*-type *Si* and selection of superlattice parameters such that transport took place in one miniband of sufficient width, it is possible to increase carrier mobility, the Seebeck coefficient and, accordingly, the TE figure of merit [78].

Note that despite a series of theoretical works on the research of TE properties of individual nanowires, at the present time there is no procedure for growing superlattices on their basis. Instead, there exists a technology for creating arrays of single-dimensional nanowires, in particular, on the basis of bismuth alloys, inside the pores of aluminum anodic samples [79].

### 3.2. Composites

Research on thermal conductivity mechanisms in superlattices has led to the conclusion that for thermal conductivity reduction a periodic structure is not mandatory. This accounted for the development of composite thermoelectric materials [80]. Nanocomposite is a bulk thermoelectric material (host) that comprises components of nanometer scale. Introduction of many surfaces into host

material allows due to scattering surface to reduce the thermal conductivity, as well as with the help of energy filtration of carriers or quantum restriction to increase the Seebeck coefficient  $S$ . In so doing, growth of  $S$  must compensate with excess the electrical conductivity reduction, thereby increasing the TE power factor. Such materials are easily processed and can be united into a series of desirable shape to be used in the instruments. Due to their design, nanocomposites must have a lower thermal conductivity than the alloys with the same rated composition of components.

Different research groups proposed various procedures for synthesis and processing of these materials [81, 82] that are united by a series of general fundamental concepts but differ in the details of their implementation. For instance, for the preparation of nanoparticles one employs the wet chemistry or ball milling methods, or the inert gas condensation method [83]. Thus, for  $Si_xGe_{1-x}$  alloy the prepared nanometer particles of  $Si$  and micrometer particles of  $Ge$  were pressed in the hot state under a pressure of plasma or in argon at 1333 K. This procedure made it possible to obtain hard, mechanically strong bulk nanocomposites with a density close to theoretical. In this way, a disc of diameter 2.54 cm and samples of other shapes were prepared. To control the integrity of nanoparticles during all processing stages, use was made of XRD-method technology, scanning electron microscopy (SEM) and transmission electron microscopy (TEM). Such investigations confirmed the previous theoretical predictions of the importance of attainment in the experimental sample of TE nanocomposite density close to theoretical, especially with regard to nanometer particles [83].

Model calculations that are used for the selection of optimal technological parameters in the course of preparation of nanocomposite materials are based on two approaches: 1) solution of the Boltzmann equation for a unit cell that comprises aligned nanoparticles with periodical boundary conditions introduced with regard to thermal flux direction and with a fixed temperature difference through each cell, as well as with surface reflectivity and relaxation time used as input parameters [80]; 2) the Monte-Carlo method is also employed in the case of disordered size, orientation and particle distribution [84]. Such calculations show that in  $Si_xGe_{1-x}$  nanocomposites in the range of  $0.2 < x < 0.8$ , when nanoparticles have a size of order 10 nm, the thermal conductivity can be considerably reduced as compared to alloy of the same composition. Besides, with increasing the volume fraction of  $Si$  nanoparticles in  $Ge$  host material, there is a drop in thermal conductivity which is completely different from  $Si_xGe_{1-x}$  alloy where the thermal conductivity grows with increasing  $Si$  concentration [85]. This is explained by the fact that nanoparticle size 50 nm and less creates the respective restriction for mean free path, so thermal conductivity  $\kappa$  becomes more sensitive to sound velocity and specific heat. With increasing the volume fraction of  $Si$ , the main mechanism for reduction of silicon effective thermal conductivity is scattering [85].

Apart from composites with a disordered distribution of nanoparticles which, when sufficiently small-sized, can be considered to be quantum dots, there are also composites with randomly distributed nanowires. According to calculations,  $Si-Ge$  nanocomposites with  $Si$  wire diameter (10 – 50) nm can have a lower thermal conductivity than in  $Si-Ge$  superlattices (polylayers) with the same film thickness and in the same  $Si_xGe_{1-x}$  stoichiometry (at  $x > 0.60$ ) [86]. This indicates the possibility of substitution of expensive superlattices by cost-effective nanocomposites having a lower thermal conductivity. Fig. 8 shows a dependence of thermal conductivity on the interface area per unit volume of  $Si$  nanoparticles and nanowires in  $Ge$  host material obtained by Monte-Carlo simulation [1]. The value of minimum thermal conductivity was taken from work [87]. As can be seen, when the interface area per unit volume exceeds  $0.08 \text{ nm}^{-1}$ , the nanocomposite thermal conductivity is lower than in the bulk alloy for the same sample types. These results testify to the fact that for achieving a low thermal conductivity the ordered structures are not mandatory.

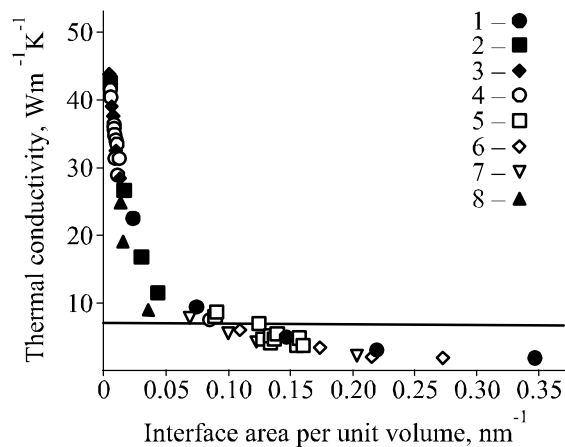


Fig. 8. Design thermal conductivity of nanostructured materials with inhomogeneities of different size and shape [1]. 1 – 3-dimensional ordered 10 nm cubic particles; 2 – 3-dimensional ordered 50 nm cubic particles; 3 – 3-dimensional ordered 200 nm cubic particles; 4 – 3-dimensional particles disordered in size and location; 5 – 3-dimensional 10 nm particles disordered in location; 6 – 3-dimensional imperfect fcc-lattice, 10 nm cubic particles; 7 – 2-dimensional ordered 10 nm nanowires; 8 – 2-dimensional ordered 50 nm nanowires.

A theoretical model constructed in work [88] has shown that short-wave phonons in a nanocomposite are mainly scattered on point defects of host material, whereas nanoparticles scatter phonons with the average and long wavelengths. In the same work for  $In_{0.53}Ga_{0.47}As$  alloy with  $ErAs$  inclusions there was experimentally revealed a considerable reduction of thermal conductivity and, hence, the TE figure of merit increase of this material by a factor of two. A reduction of thermal conductivity was also recorded for  $Zr_{0.5}Hf_{0.5}Ni_{0.8}Pd_{0.2}Sn_{0.99}Sb_{0.01}$  nanocomposite from  $3.6 \text{ W(m}\cdot\text{K)}^{-1}$  in the absence and to  $2.5 \text{ W(m}\cdot\text{K)}^{-1}$  in the presence of a volume fraction of  $ZrO_2$  particles at  $T = 700 \text{ K}$ . In so doing, the increase in volume fraction of  $ZrO_2$  particles lead to growth of the Seebeck coefficient modulus and to the TE figure of merit  $ZT = 0.75$ . It was established that thermal conductivity of nanostructured  $Si$  samples with granule size 10 – 30 nm was reduced by an order with regard to the bulk silicon, and introduction of 5% of  $Ge$  atoms reduced thermal conductivity by another factor of 2 to the value of  $5 - 6 \text{ W(m}\cdot\text{K)}^{-1}$ . The TE figure of merit of such  $Si_{0.95}Ge_{0.05}$  sample was 0.95 at 900 K [89]. Doping of  $PbTe$  with silver and antimony results in formation of  $AgPb_{2n}SbTe_{2n+2}$  compound together with nanosized  $AgSb$  inclusions, which eventually yields  $ZT = 2.2$  at 800 K [90]. Growth of  $S$  and reduction of thermal conductivity  $\kappa$  is also observed in sintered polycrystalline samples of  $n$ -type  $PbTe$  with grain size reduction from 4 to 0.7  $\mu\text{m}$  [91]. The same is observed in nanogranulated  $PbTe$  samples with grain size (30 – 50) nm.

Note that at room temperatures the TE figure of merit of nanocomposites remains very low as compared to superlattices, so intensive efforts are being pursued in this direction now.

### 3.3. Nanoobjects: quantum wells, quantum wires and quantum dots

Research on individual nanoobjects in thermoelectricity is faced with a number of objectives. First, study of thermoelectric characteristics of an individual quantum well allows selecting optimal characteristics of a superlattice with rather high barriers in the case of transport along the plane of its layers. The same can be said of a quantum wire in quantum wire arrays of certain matrix. Information on the optimal geometrical characteristics of an individual nanowire can be used for synthesis of composites with their random distribution. Besides, it is important to understand transport in nanostructures with a periodical sequence of quantum dots. Also, a need in such studies is caused by purely scientific interest in quantum size effects and scattering processes in nanostructures.

The authors of [92] performed a systematic theoretical analysis of electron states and transport processes in the  $n$ -type  $PbTe/Pb_{1-x}Eu_xTe$  quantum wells. In so doing, carrier scattering on the optical and acoustic phonons was taken into account. With regard to intersubband transitions, a variation method was used to solve the kinetic equations and determine the dependences of thermoelectric parameters on the well width for QW structures with crystallographic orientations [100] and [111] and

with different charge densities. It was established that power factor ( $S^2\sigma$ ) is larger for QW with orientation [100]. In so doing, a reduction in potential barrier ( $U$ ), with a constant charge density, leads to a reduction of power factor. However, the latter can be increased due to increase in allowed carrier concentration. Hence, at  $U = 250$  meV,  $d = 20$  Å,  $n = 5 \cdot 10^{18}$  cm<sup>-3</sup> the expected values of power factor are  $175 \mu\text{Wcm}^{-1}\text{K}^{-2}$  and  $108 \mu\text{Wcm}^{-1}\text{K}^{-2}$  for orientations [100] and [111], respectively. Experimental validation of previously obtained results for  $d$ -dependences of thermoelectric parameters of QW [111]  $\text{PbTe}/\text{Pb}_{1-x}\text{Eu}_x\text{Te}$  with  $x = 0.073$  ( $U = 171$  meV) at 300 K is given in [93]. In this work, a reduction of power factor with growing potential barrier height from  $U = 171$  meV to  $U = 250$  meV with a constant concentration of  $n$  is recorded. This effect is attributable to drop of  $\sigma$  and  $S$  which is due to more localized wave functions in a deeper potential well. However, in deeper wells a possibility emerges to raise the optimal density of carriers. Certain discrepancy between the experimental and calculated data is attributable to the emergence of a new subband close to the height of potential barrier which appears at  $d = 50$  Å, and since a continuous spectrum is not taken into account, calculations for this  $d$  are less precise. In [94] solution of kinetic equations by iterations method allowed analysing the thermoelectric figure of merit of  $\text{PbTe}/\text{Pb}_{1-x}\text{Eu}_x\text{Te}$  QW in a wide range of well widths and carrier concentrations (Fig. 9). As is apparent, at maximum carrier concentration ( $n = 10^{19}$  cm<sup>-3</sup>) and with orientation [100],  $ZT$  attains the value of 1.3 at  $T = 300$  K.

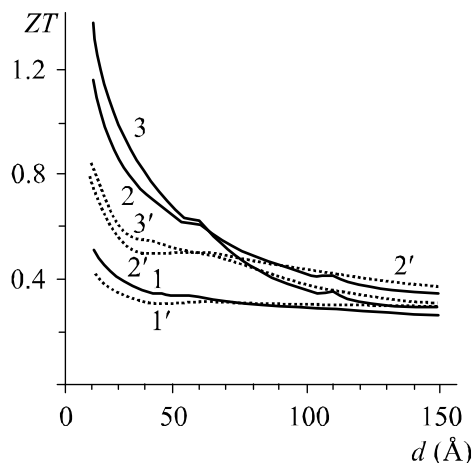
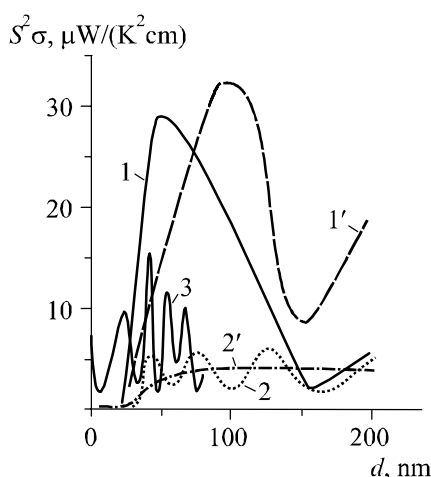


Fig. 9. Dependence of thermoelectric figure of merit of  $\text{PbTe}/\text{Pb}_{1-x}\text{Eu}_x\text{Te}$  quantum wells on the well width for [100] (curves 1, 2, 3) and [111] (curves 1', 2', 3') orientations. Carrier concentration  $n$ , cm<sup>-3</sup>:  $10^{18}$  – curves 1, 1';  $5 \cdot 10^{18}$  – curves 2, 2';  $10^{19}$  – curves 3, 3',  $T = 300$  K [94].

Due to the complexity of measuring thermal conductivity of thin films, the experimental works on measuring their TE parameters are often restricted to thermoelectric power factor  $S^2\sigma$ . Comparison of thickness dependences of  $S^2\sigma$  in IV – VI thin films shows that the highest value of this coefficient  $S^2\sigma \approx 90 \mu\text{Wcm}^{-1}\text{K}^{-2}$  can be achieved in  $\text{PbSe}$  films [58-63]. Besides, works [62, 66] experimentally support the above theoretical predictions as to  $S^2\sigma$  increase due to growth of major carrier concentration. In work [62] the concentration of  $n$ -type carriers in  $\text{PbTe}$  films was increased due to  $\text{Pb}$  excess in the output batch, and in [66] – by doping of lead telluride with bismuth. Although  $\text{PbTe}$  films doped with  $\text{Bi}$  were not protected from oxidation, maximum  $S^2\sigma$  values in both cases proved to be commensurate ( $S^2\sigma \approx 30 \mu\text{Wcm}^{-1}\text{K}^{-2}$ ). Such  $S^2\sigma$  value proves to be larger than in other known nanostructures based on  $\text{PbTe}$  and  $\text{Bi}$  (Fig. 10).

Here regard must be paid to the following. The oscillation periods of TE parameters in QW theoretically calculated by the known Fermi energy for the bulk samples not always coincide with those determined experimentally. This, in particular, can be related to model oversimplification: failure to take into account the presence of impurities and other defects both on the surface and in the bulk, the anisotropy of energy levels and nonparabolic dependence of charge carrier energy on quasi-impulse. Besides, the model does not take into account the specific layered structure and the nonidentity of barriers at the interfaces.



*Fig. 10. Dependences of thermoelectric power factor  $S^2\sigma$  on the layer thickness: stoichiometric (curve 1) and with 2 at.% of excess lead (curve 1') PbTe in KCl/n-PbTe/EuS nanostructure [62]; Bi grown at  $T_{n1} = 380$  K (curve 2) and  $T_{n2} = 300$  K (curve 2') in mica/n-Bi/EuS structure [54]; and Bi in mica/PbTe/Bi/Al<sub>2</sub>O<sub>3</sub> heterostructure ( $d_{PbTe} = 50$  nm) (curve 3) [54] at  $T = 300$  K.*

As regards quantum wires, as previously mentioned, the greatest promise in this area is shown by bismuth based materials. Theoretical calculations show that a reduction of nanowire diameter leads to growth of its  $ZT$ . In particular, in [95] it is shown that with a diameter of 5 Å in  $Bi_2Te_3$  wire at room temperature  $ZT = 14$ . These results were confirmed in theoretical works [96, 97] for  $Bi$  quantum wire. Note that calculations in all these works were performed in the approximation of constant relaxation time. In theoretical works [98, 99] for free  $GaAs$  and  $Si$  nanowires there was revealed a reduction of its thermal conductivity with a decrease in diameter. Calculations [99, 100] for III – V and II – VI semiconductors showed that the reduction value of nanowire thermal conductivity against the bulk samples depends on the ratio of atomic masses of compound components. In so doing, the largest value of thermoelectric figure of merit  $ZT \approx 6$  can be achieved in free  $InSb$  and  $InAs$  quantum wires (Fig. 11) [101, 102].

Experimental investigations of the temperature dependence of the electrical resistivity of  $Bi$  nanowires of diameter 9 and 15 nm in aluminum oxide matrix show that such samples possess semiconductor properties with the energy gap width 0.17 – 0.4 eV. The Seebeck coefficient at room temperature proved to be higher in the samples of diameter 9 nm and made  $2 \cdot 10^4 \mu V \cdot K^{-1}$ . The thermoelectric figure of merit of pressed powder of  $Bi_2Te_3$  nanotubes obtained by hydrothermal synthesis at  $T = 450 - 500$  K is approximately equal to unity [103]. Measuring the TE figure of merit of easy to produce silicon nanowires of diameter 20 – 300 nm due to their thermal conductivity reduction by two orders against the bulk samples gave the value of  $ZT \approx 0.6$  at room temperature [104].

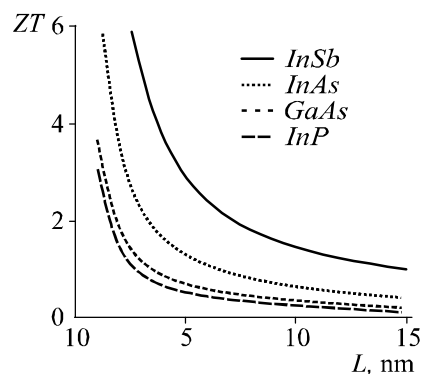


*Fig. 11. Dependence of design figure of merit  $ZT$  on the diameter of  $InSb$ ,  $InAs$ ,  $GaAs$  and  $InP$  nanowires [102].*

Works [105 – 108] demonstrate the possibility of experimental synthesis of quantum dot superlattices along nanowires (other names: quantum dot stacks, superlattices in quantum wire), and in

work [109] calculations were made with indication of parameters that must be controlled to improve the operating efficiency of this superlattice type. It was established that owing to diameter-independent subband energy, potential barrier regions and the bulk heterostructure wells can be inverted into quantum dot stacks. In so doing, the dependence of thermoelectric figure of merit  $ZT$  on nanowire segment length is of a nonmonotonic oscillation nature (Fig. 12). It is seen that the optimal segment length of  $n$ - $PbSe/PbS$  quantum dot stack is nearly 3 nm for both orientations [001] and [111] with  $ZT$  value 4.4 and 3.7, respectively (Fig. 12, a). Note that  $p$ - and  $n$ -type quantum dot stacks of respective diameters have a similar dependence of  $ZT$  on segment length (Fig. 12 a, b). In so doing,  $ZT$  for  $p$ - $PbSe/PbS$  quantum dot stacks is 6.2 and 4.4 with segment lengths  $\sim 2$  nm and  $\sim 4$  nm for [001] and [111] orientations, respectively (Fig. 12, b). The  $p$ - $PbSe/PbS$  quantum dot stacks have somewhat higher  $ZT$  value than  $n$ -type wires (Fig. 12 a, b). The reason for this can be a lower effective mass of holes than of electrons in  $PbSe$  and  $PbS$ . From Fig. 12, c it is seen that for  $n$ - $PbSe/PbTe$  quantum dot stacks of diameter 10 nm the oscillation behaviour is less pronounced than for 5 nm. For these quantum dot stacks of diameter 5 nm the optimal  $ZT$  values are 6.4 and 8.1 for segments of length 2 nm and for both orientations [001] and [111] (Fig. 12, c). In general, it can be noted that  $PbSe/PbTe$  quantum dot stacks possess better thermoelectric figure of merit than their  $PbSe/PbS$  analogs, which is attributable to larger carrier anisotropy and lower effective masses of  $PbTe$  than in  $PbS$ , which assure a larger density of states and lower effective masses in nanowires than in the bulk materials [109].

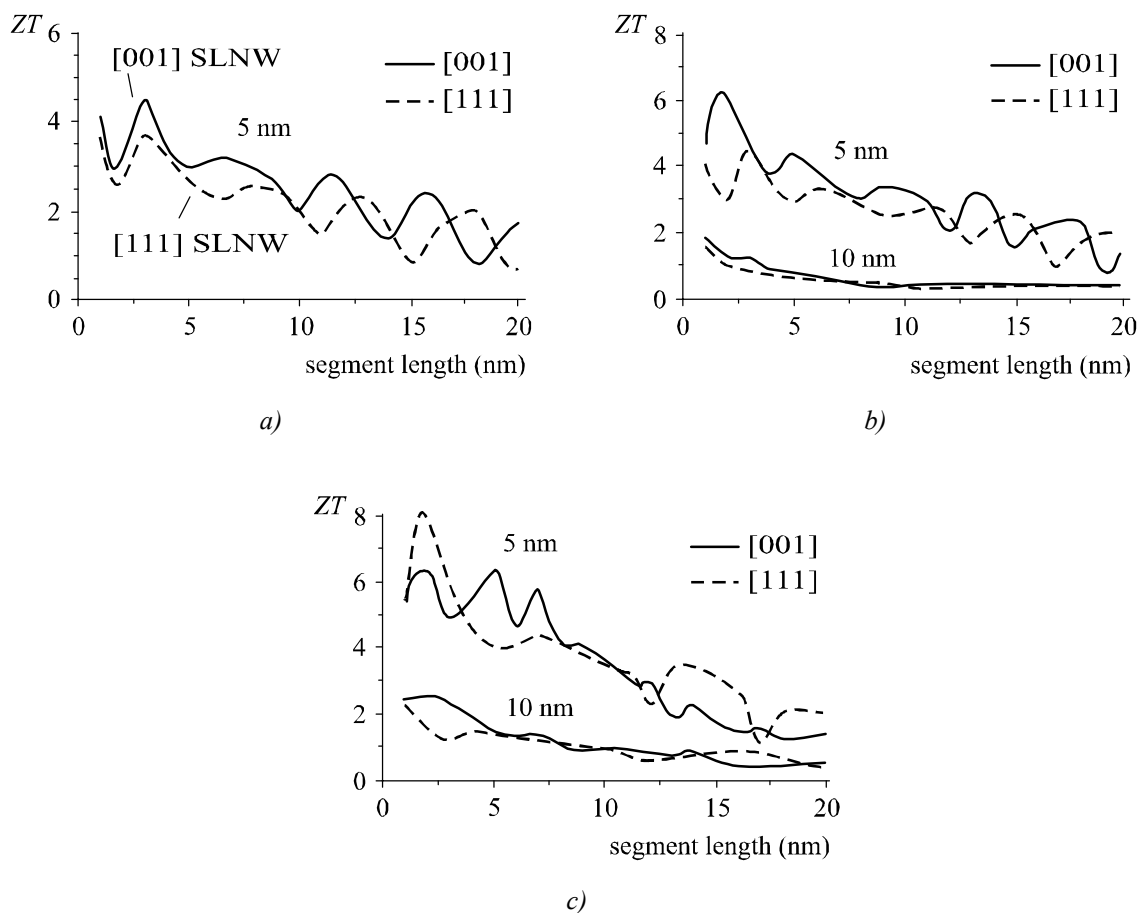


Fig. 12. Dependence of thermoelectric figure of merit  $ZT$  of  $n$ - $PbSe/PbS$  (a),  $p$ - $PbSe/PbS$  (b) and  $n$ - $PbSe/PbTe$  (c) nanowire superlattices of different diameters on heterostructure segment length for [001] (—) and [111] (---) orientations at 77 K [109].

In 2010 in the theoretical works by V. Fomin and P. Kratzer there was revealed high sensitivity of  $ZT$  coefficient to the Fermi energy value and, respectively, to carrier concentration in *InAs/GaAs* quantum dot stacks. Thus, at certain Fermi energy values the  $ZT$  value of *InAs/GaAs* quantum dot stacks is almost equal to zero, and at other values, rather close to previous ones, the thermoelectric figure of merit reaches the value of  $ZT = 3$  [110, 111].

## Conclusions

This paper is a review of the basic theoretical and experimental works dedicated to the influence of quantum size effects on the thermoelectric properties of nanostructured materials. The main strategies and concepts in this direction are highlighted. It is shown that the main factor for revival of interest in thermoelectricity in the early 90-s was the possibility of thermoelectric figure of merit improvement due to material size reduction. Experimental measurements of the TE figure of merit of superlattices based on quantum wells and dots, composites based on quantum wires and dots, nanowire arrays, as well as individual nanoobjects have partially confirmed previous theoretical foresights.

To understand the ways for thermoelectric figure of merit enhancement, the main objective today lies in the development of theoretical models of influence of quantum size effects on the electron and phonon subsystems of nanostructures. The prerequisite for achievement of desirable thermoelectric figure of merit is development of a technique for fabrication of nanostructures with the assigned average size of particles, their distribution according to size and density that should be maintained during creation and processing, as well as in operation.

The work was performed within the state budget scientific research project № 0111U001766 of the Ministry of Education and Science, Youth and Sports of Ukraine, the State Foundation for Fundamental Research, the State Agency for Science, Innovation and Information of Ukraine № 0110U007674 and the National Academy of Sciences of Ukraine № 0110U006281.

## References

1. M.S. Dresselhaus, G. Ghen, M.I. Rang, R. Yang, H. Lee, D. Wang, Z. Ren, J.-P. Fleurial and P. Gogna, New Directions for Low-Dimensional Thermoelectric Materials, *Adv. Mater.* **19**, 1043-1053 (2007).
2. A.V. Dmitriyev, I.P. Zvyagin, Modern Trends in the Development of Physics of Thermoelectric Materials, *Uspekhi Fiz.Nauk* **180** (8), 821-838(2010).
3. H. Ohta, Thermoelectrics Based on Strontium Titanate, *Materials Today* **10**, 44-49 (2007).
4. V.M. Shperun, D.M. Freik and R.I. Zapukhlyak, *Thermoelectricity of Lead Telluride and its Analogs* (Plai, Ivano-Frankivsk, 2000).
5. T.M. Tritt, M.A. Subramanian, Thermoelectric Materials, Phenomena, and Applications: A Bird's Eye View, *MRS Bulletin* **31**, 188-198 (2006).
6. Y.-M. Lin, S.B. Cronin, J.Y. Ying, M.S. Dresselhaus and J.P. Heremans, Transport Properties of *Bi* Nanowire Arrays, *Appl. Phys. Lett.*, **76**, 3944 (2000).
7. L.D. Hicks, T.C. Harman, X. Sun and M.S. Dresselhaus, Experimental Study of the Effect of Quantum-Well Structures on the Thermoelectric Figure of Merit, *Phys. Rev. B: Condens. Matter Mater. Phys.*, **53** (16), R10493 (1996).
8. T. Koga, S.B. Cronin, M.S. Dresselhaus, J.L. Liu, K.L. Wang, Experimental Proof-of-Principle Investigation of Enhanced  $Z_{3D}T$  in (001) Oriented *Si/Ge* Superlattices, *Appl. Phys. Lett.*, **77**, 1490 (2000).
9. T.C. Harman, P.J. Taylor, D.L. Spears and M.P. Walsh, *Proc. of the 18th Int. Conf. on*

- Thermoelectrics* (AIP, New York, 1999).
10. R. Venkatasubramanian, *Recent Trends in Thermoelectric Materials Research III* (Ed. by T.M. Tritt): Semiconductors and Semimetals, Vol. 71 (Chapter 4, pp. 175-201) (Academic, New-York, 2001).
  11. B. Yang, G. Chen, *Beyond Bismuth Telluride in Chemistry, Physics, and Materials Science for Thermoelectric Materials* (Kluwer Academic/Plenum Publisher, New York, 2003).
  12. T.E. Humphrey, M.F. O'Dwyer and H. Linke, Power Optimization in Thermionic Devices, *J. Phys. D: Appl. Phys.*, **38**, 2051 (2004).
  13. Y.I. Ravich, *CRC "Handbook of Thermoelectrics"* (Ed: DM Rowe) (CRC Press, New York, 1995).
  14. T. Koga, X. Sun, S.B. Cronin and M.S. Dresselhaus, Carrier Pocket Engineering to Design Superior Thermoelectric Materials Using *GaAs/AlAs* Superlattices, *Appl. Phys. Lett.* **73**, 2950 (1998).
  15. P.Y. Yu, M. Cardona, *Fundamentals of Semiconductors – Physics and Material Properties*. – 3rd edition (Springer, Berlin, 2001), p.22.
  16. T. Koga, X. Sun, S.B. Cronin and M.S. Dresselhaus. Carrier Pocket Engineering Applied to “Strained” *Si/Ge* Superlattices to Design Useful Thermoelectric Materials, *Appl. Phys. Lett.*, **75**, 2438 (1999).
  17. Y.-M. Lin, M.S. Dresselhaus and J.Y. Ying, *Advances in Chemical Engineering* (Ed. by K. Ricci) (Academic, York, PA, 2001), Ch.5, pp. 167 – 203.
  18. S. Takaoka, K. Murase, Studies of Far-Infrared Properties of Thin Bismuth Films on *BaF<sub>2</sub>* Substrate, *J. Phys. Soc. Jpn.*, **54**, 2250 (1985).
  19. J. Heremans, C.M. Thrush, Y.-M. Lin, S. Cronin, Z. Zhang, M.S. Dresselhaus and J.F. Mansfield, Bismuth Nanowire Arrays: Synthesis and Galvanomagnetic Properties, *Phys. Rev. B: Condens. Matter Mater. Phys.*, **61**, 2921 (2000).
  20. L.D. Hicks, T.C. Harman and M.S. Dresselhaus, Use of Quantum Well Superlattices to Obtain a High Figure of Merit from Nonconventional Thermoelectric Materials, *Appl. Phys. Lett.*, **63**, 3230(1993).
  21. J. Heremans, C.M. Thrush, D.T. Morelli and M.-C. Wu, Resistance, Magnetoresistance, and Thermopower of Zinc Nanowire Composites, *Phys. Rev. Lett.* **91**, 076804 (2003).
  22. I.M. Lifshits, A.M. Kosevich, *Doklady AN SSSR* **91**, 795 (1953).
  23. I.M. Lifshits, A.M. Kosevich, On the Oscillations of Thermodynamic Values for the Degenerate Fermi-Gas at Low Temperatures, *Izvestia AN SSSR. Ser. Fizika* **19**, 395 (1955).
  24. A.M. Kosevich, I.M. Lifshits, The de Haas-van Alphen Effect in Thin Metal Layers, *JETF* **29**, 743 (1955).
  25. I.M. Lifshits, M.I. Kaganov, *Uspekhi Fiz. Nauk* **69**, 419(1959).
  26. V.B. Sandomirsky, Towards the Theory of Quantum Effects in the Electrical Conductivity of Semiconductor Films, *Radiotekhnika i Radioelektronika*, **7**, 1971 (1962).
  27. V.B. Sandomirsky, Dependence of the Energy Gap Width in Semiconductor Films on Their Thickness and Temperature, *JETF* **43**, 2309 (1962).
  28. B.A. Tavger, V.Ya. Demikhovskiy, Some Effects Caused by Discreteness of Electron Energy Spectrum in Thin Films, *Fizika Tverdogo Tela* **5**(2), 644-648 (1963).
  29. Yu.F. Ogrin, V.N. Lutsky and M.I. Elinson, Observation of Quantum Size Effects in *Bi* Films, *Letters to JETF* **3**, 114-118 (1966).
  30. V.N. Lutsky, D.N. Korneyev and M.I. Elinson, Observation of Quantum Size Effects in Bismuth Films via Tunneling Spectroscopy Method, *Letters to JETF* **4**, 267-270 (1966).
  31. B.A. Tavger, V.Ya. Demikhovskiy, Quantum Size Effects in Semiconductor and Semimetal Films, *Uspekhi Fiz. Nauk* **96**(1), 61-86 (1968).
  32. V.B. Sandomirsky, Quantum Dimensional Effect in Semimetal Film, *JETF* **52**, 158 (1967).
  33. M.I. Kaganov, S.S. Nedorezov and A.M. Rustamova, Towards the Theory of Quantum Size

- Effects, *Fiz.Tverdogo Tela* **12**, 2277 (1970).
34. V.N. Lutsky, Peculiarities of Optical Absorption of Metal Films in Metal to Dielectric Conversion Region, *Letters to JETF* **2**, 391-395 (1965).
  35. E.I. Bukhshtab, Yu.F. Komnik and Yu.V. Nikitin, Semimetal-Semiconductor Transition with a Change in Thickness of Bismuth-Antimony Alloy Films, *Fizika Nizkikh Temperatur* **8**(5), 513-517(1982).
  36. G.A. Gogadze, I.O. Kulik, Tunneling Current Oscillations from Thin Metal Layers, *Fizika Tverdogo Tela* **7**, 432 (1965).
  37. E.T. Rogovskaya, Effect of Dimensional Quantization on the Conductivity in Metal-Oxide-Semiconductor Systems, *Fiz. i Tekhn.Polupr.***7**, 1209 (1973).
  38. F. Malone, W.D. Deering, The Role of Defects in the Quantum Size Effect, *Thin Solid Films* **27**, 177 (1975).
  39. E.M. Baskin, A.V. Chaplik, M.V. Entin, Localized Electron States in Thin Layers Caused by Geometric Surface Defects, *JETF* **63**, 1077 (1972).
  40. A.V. Chaplik, The Impurity Scattering of Electrons in Quantizing Films, *JETF* **59**, 2110 (1970).
  41. B.M. Askerov, *Electron Transport Effects in Semiconductors* (Nauka, Moscow, 1985).
  42. A.Ya. Shik, G.B. Bakuyeva and S.F. Musikhin, *Physics of Nanodimensional Systems* (Nauka, Saint-Petersburg, 2001).
  43. Yu.F. Konmik, E.I. Bukhshtab, Quantum Size Effects in Thin Tin Films, *Letters to JETF* **8**, 9-13 (1968).
  44. N.E. Alekseevskii, S.I. Vedeneev, Dependence of the Transparency of Aluminum on the Thickness, *Letters to JETF* **6**(9), 865-868 (1967).
  45. M.L. Dmytruk, O.S. Kondratenko, S.A. Kovalenko and I.B. Mamontova, Classical and Topological Size Effects in the Optical Properties of Gold Thin Films, *Fizyka i Khimiya Tverdogo Tila* **7**(1), 39-44 (2006).
  46. R.I. Bigun, Z.V. Stasyuk, Transition from Quantum to Classical Charge Transport in Copper Thin Films, *Fizyka i Khimiya Tverdogo Tila* **6**(3), 414-417 (2005).
  47. Yu.F. Komnik, V.V. Andrievsky and E.I. Bukhshtab, Features of Magnetoresistance in Bismuth Thin Films, *Fizika Tverdogo Tela* **12**(11), 3266-3269 (1970).
  48. Yu.F. Ogrin, V.N. Lutsky, R.M. Sheftal, M.U. Arifova and M.I. Elinson, Quantum Size Effects in Bismuth Thin Films, *Radiotekhnika i Radioelektronika* **12**, 748 (1967).
  49. Yu.F. Konmik, E.I. Bukhshtab, Observation of Quantum and Classical Size Effects in Polycrystalline Bismuth Thin Films, *JETF* **54**(1), 63-68 (1968).
  50. Yu.F. Konmik, E.I. Bukhshtab and Yu.V. Nikitin, Quantum Size Effect in Bismuth Thin Films Doped with Antimony, *Fizika Nizkikh Temperatur* **1**(2), 243-246 (1975).
  51. Yu.F. Konmik, E.I. Bukhshtab, Detection of Quantum Oscillations of Conductivity in Antimony Thin Films, *Letters to JETF* **6**, 536-540 (1967).
  52. Yu.F. Konmik, E.I. Bukhshtab and Yu.V. Nikitin, V.V. Andriyevskiy, Peculiarities of Temperature Dependence of Resistance in Bismuth Thin Films, *JETF* **60**(2), 669-687 (1971).
  53. V.N. Lutsky, L.A. Kulik, Peculiarities of Optical Characteristics of Bismuth Films Under Quantum Size Effect, *Letters to JETF* **8**, 133-137 (1968).
  54. S.G. Lyubchenko, Transport and Quantum Size Effects in Lead Telluride and Bismuth Thin Films and Structures on Their Basis, *Synopsis of Ph.D. Thesis in Physics and Mathematics: Specialty 01.04.10 "Physics of Semiconductors and Dielectrics"* (Kharkiv, 2007).
  55. O.N. Filatov, I.A. Karpovich, Quantum Size Effects in *InSb* Thin Films, *Letters to JETF*, **10**, 224-

- 226 (1969).
56. D.M. Freik, I.K. Yurchishin, V.V. Bachuk, L.T. Kharun, Yu.V. Lysyuk, Thermoelectric Properties of *PbTe* Thin Films Exposed to Air, *Fizyka i Khimiya Tverdogo Tila* **11** (3), 598-603 (2010).
  57. Yu.V. Klanichka, B.S. Dzundza, L.T. Kharun and G.D. Mateik, Effect of Oxygen on the Electric Parameter Profiles of Lead Telluride Single-Crystal Films, *Fizyka i Khimiya Tverdogo Tila* **10**(2), 303-306 (2009).
  58. E.I. Rogacheva, I.M. Krivulkin, O.N. Nashchekina, A.Yu. Sipatov, V.V. Volobuev and M.S. Dresselhaus, Effect of Oxidation on the Thermoelectric Properties of *PbTe* and *PbS* Epitaxial Films, *Applied Physics Letters* **78** (12), 1661-1663 (2001).
  59. E.I. Rogacheva, T.V. Tavrina, O.N. Nashchekina, S.N. Grigorov and K.A. Nasedkin, Quantum Size Effects in *PbSe* Quantum Wells, *Applied Physics Letters* **80** (15), 2690-2692 (2002).
  60. E.I. Rogacheva, O.N. Nashchekina, Y.O. Vekhov, M.S. Dresselhaus and S.B. Cronin, Effect of Thickness on the Thermoelectric Properties of *PbS* Thin Films, *Thin Solid Films* **423**, 115–118 (2003).
  61. E.I. Rogacheva, I.M. Krivulkin, O.N. Nashchekina, A.Yu. Sipatov, V.A. Volobuev and M.S. Dresselhaus, Percolation Transition of Thermoelectric Properties in *PbTe* Thin Films, *Appl. Phys. Lett.* **78** (21), 3238–3240 (2001).
  62. E.I. Rogacheva, O.N. Nashchekina, S.N. Grigorov, M.S. Dresselhaus and S.B. Cronin, Oscillatory Behaviour of the Transport Properties in *PbTe* Quantum Wells, *Institute of Physics Publishing. Nanotechnology* **14**, 53–59 (2003).
  63. E.I. Rogacheva, O.N. Nashchekina, A.V. Meriuts, S.G. Lyubchenko, M.S. Dresselhaus and G. Dresselhaus, Quantum Size Effects in *n-PbTe/p-SnTe/n-PbTe* Heterostructures, *Applied Physics Letters* **86**, 063103 (2005).
  64. E.I. Rogacheva et al, Oscillations in the Thickness Dependences of the Room-Temperature Seebeck Coefficient in *SnTe* Thin Films, *Thin Solid Films* **484**(1-2), 433-437 (2005).
  65. I.K. Yurchishin, I.I. Chavyak, Yu.V. Lysyuk, L.T. Kharun, Size Effects in Thermoelectric Parameters of Tin Telluride Nanostructures, *Fizyka i Khimiya Tverdogo Tila* **11** (4), 898-903 (2010).
  66. D.M. Freik, I.K. Yurchishin, Yu.V. Lysyuk, G.D. Mateik and O.R. Nadruga, Quantum Size Effects of Thermoelectric Parameters of *PbTe* and *Bi* Based Nanostructures, *Fizyka i Khimiya Tverdogo Tila* **12** (3), 650-655 (2011).
  67. D.M. Freik, I.K. Yurchishin, V.M. Chobanyuk, R.I. Nikiruy and Yu.V. Lysyuk, Nanostructures Based on IV-VI Compounds for Thermoelectric Power Converters, *Sensorna Elektronika ta Microsystemni Tekhnologii* **2** (8), 41-54 (2011).
  68. V. Narayanamurti et al., Selective Transmission of High-Frequency Phonons by a Superlattice: The "Dielectric" Phonon Filter, *Phys. Rev. Lett.* **43**, 2012 (1979).
  69. S-M. Lee, D.G. Cahill and R. Venkatasubramanian, Thermal Conductivity of *Si-Ge* Superlattices, *Appl. Phys. Lett.* **70**, 2957 (1997).
  70. M.N. Touzelbaev et al, Thermal Characterization of *Bi<sub>2</sub>Te<sub>3</sub>/Sb<sub>2</sub>Te<sub>3</sub>* Superlattices, *J. Appl. Phys.* **90**, 763 (2001).
  71. R. Venkatasubramanian, Lattice Thermal Conductivity Reduction and Phonon Localization-Like Behavior in Superlattice Structures, *Phys. Rev. B.* **61**, 3091 (2000).
  72. E.S. Landry, M.I. Hussein and A.J.H. McGaughey, Complex Superlattice Unit Cell Designs for Reduced Thermal Conductivity, *Phys. Rev. B.* **77**, 184302 (2008).
  73. A.V. Dmitriev, R. Keiper and V.V. Makeev, Electron Spectrum and Infrared Transitions in Semiconductor Superlattice with a Unit Cell Allowing for Quasi-Localized Carrier States, *Physica E* **11**, 391 (2011).

74. A. Khitun et al., In-Plane Lattice Thermal Conductivity of a Quantum-Dot Superlattice, *J. Appl. Phys.* **88**, 696 (2000).
75. T.C. Harman et al., Quantum Dot Superlattice Thermoelectric Materials and Devices, *Science* **297**, 2229 (2002).
76. T.C. Harman, M.P. Walsh, B.E. LaForge and G.W. Turner, Nanostructured Thermoelectric Materials, *J. of Electronic Mater.* **34** (5), L19L22 (2005).
77. T.C. Harman, P.J. Taylor, M.P. Walsh and B.E. LaForge, Quantum Dot Superlattice Thermoelectric Materials and Devices, *Science* **297**, 2229 (2002).
78. A.A. Balandin, O.L. Lazarenkova, Mechanism for Thermoelectric Figure-of-Merit Enhancement in Regimented Quantum Dot Superlattices, *Appl. Phys. Lett.* **82**, 415 (2003).
79. Yong Peng, Dong-Huan Qin, Rong-Lie Zhou and Hu-Lin Li, Bismuth Quantum-Wires Arrays Fabricated by Electrodeposition in Nanoporous Anodic Aluminum Oxide and Its Structural Properties, *Materials Science and Engineering B* **77**, 246–249 (2000).
80. R.G. Yang, G. Chen, Thermal Conductivity Modeling of Periodic Two-Dimensional Nanocomposites, *Phys. Rev. B: Condens. Matter Mater. Phys.* **69**, 195316 (2004).
81. J.P. Heremans, Materials and Technologies for Direct Thermal-to-Electric Energy Conversion, *MRS Symp.Proc.* (Materials Research Society Press, Pittsburgh, 2005, P. 0886-F04-10.1).
82. A. Shakouri, Thermoelectric Materials 2005 - Research and Applications, *MRS Symp. Proc.* (Materials Research Society Press, Pittsburgh, 2005, P. F7.1).
83. M.S. Dresselhaus, G. Chen, M.Y. Tang, R.G. Yang, H. Lee, D.Z. Wang, Z.F. Ren, J.P. Fleurial and P. Gogna, Materials and Technologies for Direct Thermal-to-Electric Energy Conversion, *MRS Symp. Proc.* (Materials Research Society Press, Pittsburgh, 2005, p. 3-12).
84. M.S. Jeng, R.G. Yang, D. Song, G. Chen, Modeling the Thermal Conductivity and Phonon Transport in Nanoparticle Composites Using Monte Carlo Simulation, *J. Heat Transfer* **130**, 042410 (2008).
85. R. Yang, G. Chen and M.S. Dresselhaus, Thermal Conductivity of Simple and Tubular Nanowire Composites in the Longitudinal Direction, *Phys. Rev. B: Condens. Matter Mater. Phys.* **72**, 125418 (2005).
86. R. Yang, G. Chen, Thermal Conductivity Modeling of Periodic Two-Dimensional Nanocomposites, *Phys. Rev. B: Condens. Matter Mater. Phys.* **69**, 195316 (2004).
87. B. Abeles, Lattice Thermal Conductivity of Disordered Semiconductor Alloys at High Temperatures, *Phys. Rev.* **131**, 1906 (1963).
88. W. Kim et al., Thermal Conductivity Reduction and Thermoelectric Figure of Merit Increase by Embedding Nanoparticles in Crystalline Semiconductors, *Phys. Rev. Lett.* **96**, 045901 (2006).
89. G.H. Zhu et al, Increased Phonon Scattering by Nanograins and Point Defects in Nanostructured Silicon with a Low Concentration of Germanium, *Phys. Rev. Lett.* **102**, 196803 (2009).
90. K.F. Hsu et al, Cubic  $AgPb_mSbTe_{2+m}$ : Bulk Thermoelectric Materials with High Figure of Merit, *Science* **303**, 818 (2004).
91. K. Kishimoto, T. Koyanagi, Preparation of Sintered Degenerate *n*-type *PbTe* with a Small Grain Size and Its Thermoelectric Properties, *J. Appl. Phys.* **92**, 2544 (2002).
92. A. Casian, I. Sur, H. Scherrer and Z. Dashevsky, Thermoelectric Properties of *PbTe/PbEuTe* Quantum Wells, *Phys. Rev. B.* **61**, 15965-15974 (2000).
93. T.C. Harman, D.L. Spears and M.J. Manfra, High Thermoelectric Figures of Merit in *PbTe* Quantum Wells, *J. Electron. Mater.* **25**, 1121–1127 (1996).
94. I. Sur, A. Casian and A. Balandin, Electronic Thermal Conductivity and Thermoelectric Figure of

- Merit of *n*-type *PbTe/PbEuTe* Quantum Wells, *Phys. Rev. B.* **69**, 035306 (2004).
95. L.D. Hicks, M.S. Dresselhaus, Effect of Quantum-Well Structures on the Thermoelectric Figure of Merit, *Phys. Rev. B.* **47**, 12727 (1993).
96. X. Sun, Z. Zhang and M.S. Dresselhaus, Theoretical Modeling of Thermoelectricity in *Bi* Nanowires, *Appl. Phys. Lett.* **74**, 4005 (1999).
97. Y-M. Lin, X. Sun and M.S. Dresselhaus, Theoretical Investigation of Thermoelectric Transport Properties of Cylindrical *Bi* Nanowires, *Phys. Rev.* **62**, 4610 (2000).
98. S.G. Walkauskas et al, Lattice Thermal Conductivity of Wires, *J. Appl. Phys.* **85**, 2579 (1998).
99. N. Mingo, Calculation of *Si* Nanowire Thermal Conductivity Using Complete Phonon Dispersion Relations, *Phys. Rev. B.* **68**, 113308 (2003).
100. N. Mingo, D.A. Broido, Lattice Thermal Conductivity Crossovers in Semiconductor Nanowires, *Phys. Rev. Lett.* **93**, 246106 (2004).
101. N. Mingo, Thermoelectric Figure of Merit and Maximum Power Factor in III–V Semiconductor Nanowires, *Appl. Phys. Lett.* **84**, 2652 (2004).
102. N. Mingo, Thermoelectric Figure of Merit and Maximum Power Factor in III–V Semiconductor Nanowires, *Appl. Phys. Lett.* **88**, 149902 (2006).
103. X.B. Zhao et al, Bismuth Telluride Nanotubes and the Effects on the Thermoelectric Properties of Nanotube-Containing Nanocomposites, *Appl. Phys. Lett.* **86**, 062111 (2005).
104. A.I. Hochbaum et al, Enhanced Thermoelectric Performance of Rough Silicon Nanowires, *Nature* **451**, 163 (2007).
105. L. Piraux, J.M. George, J.F. Despres and C. Leroy, Giant Magnetoresistance in Magnetic Multilayered Nanowires, *Appl. Phys. Lett.* **65**, 2484 (1994).
106. Y. Wu, R. Fan and P. Yang, Block-by-Block Growth of Single-Crystalline Si/SiGe Superlattice Nanowires, *Nano Lett.* **2**, 83 (2002).
107. M.S. Gudiksen, L.J. Lauhon, J. Wang, D. Smith and C.M. Lieber, Growth of Nanowire Superlattice Structures for Nanoscale Photonics and Electronics, *Nature* **415**, 617 (2002).
108. M.T. Bjork, B.J. Ohlsson, T. Sass, A.I. Persson, C. Thelander, M.H. Magnusson, K. Deppert, L.R. Wallenberg and L. Samuelson, One-Dimensional Steeplechase for Electrons Realized, *Nano Lett.* **2**, 87 (2002).
109. Yu-Ming Lin, M.S. Dresselhaus, Thermoelectric Properties of Superlattice Nanowires, *Phys. Rev. B.* **68**, 075304 (2003).
110. V.M. Fomin, P. Kratzer, Thermoelectric Transport in Periodic One-Dimensional Stacks of *InAs/GaAs* Quantum Dots, *Phys. Rev. B.* **82**, 045318 (2010).
111. V.M. Fomin, P. Kratzer, Modeling of Minibands and Electronic Transport in One-Dimensional Stacks of *InAs/GaAs* Quantum Dots, *Physica E* **42**, 906-910 (2010).

Submitted 08.11.2011.